THE ASTROPHYSICAL JOURNAL, 445:927–938, 1995 June 1

THE UNUSUAL HELIUM VARIABLE AM CANUM VENATICORUM

J. L. PROVENCAL,[1,2] D. E. WINGET,[1] R. E. NATHER,[1,3] E. L. ROBINSON,[1] J.-E. SOLHEIM,[4] J. C. CLEMENS,[1,5,6] P. A. BRADLEY,[1,7] S. J. KLEINMAN,[1,8] A. KANAAN,[1] C. F. CLAVER,[1,9] C. J. HANSEN,[10] T. M. K. MARAR,[11] S. SEETHA,[11] B. N. ASHOKA,[11] E. M. LEIBOWITZ,[12] E. G. MEIŠTAS,[13] A. BRUVOLD,[4] G. VAUCLAIR,[14,15] N. DOLEZ,[14] M. CHEVRETON,[16] M. A. BARSTOW,[8,17] A. E. SANSOM,[8,17] R. W. TWEEDY,[8,18] G. FONTAINE,[15,19] P. BERGERON,[15,19] S. O. KEPLER,[20] M. A. WOOD,[21] AND A. D. GRAUER[9,22]

ABSTRACT

The unusual variable star AM CVn has puzzled astronomers for over 40 years. This object, both a photometric and spectroscopic variable, is believed to contain a pair of hydrogen-deficient white dwarfs of extreme mass ratio, transferring material via an accretion disk. We examine the photometric properties of AM CVn, analyzing 289 hours of high-speed photometric data spanning 1976 to 1992. The power spectrum displays significant peaks at 988.7, 1248.8, 1902.5, 2853.8, 3805.2, 4756.5, and 5707.8 μHz (1011.4, 800.8, 525.6, 350.4, 262.8, 210.2, and 175.2 s). We find no detectable power at 951.3 μHz (1051 s), the previously reported main frequency. The 1902.5, 2853.9, and 3805.2 μHz peaks are multiplets, with frequency splitting in each case of 20.77 ± 0.05 μHz. The 1902.5 μHz seasonal pulse shapes are identical, within measurement noise, and maintain the same amplitude and phase as a function of color. We have determined the dominant frequency to be 1902.509802 ± 0.00001 μHz, with $\dot{P} = +1.71\ (\pm 0.04) \times 10^{-11}$ s s^{-1}. We discuss the implications of these findings on a model for AM CVn.

Subject headings: accretion, accretion disks — binaries: close — stars: individual (AM Canum Venaticorum) — stars: oscillations — white dwarfs

1. INTRODUCTION

The unusual helium variable AM CVn is the prototype of a special class of ultra–short-period interacting binaries, which provide an exciting avenue to explore nucleosynthesis, binary star evolution, and stellar structure. Interacting binary white dwarfs (IBWDs) contain two helium white dwarfs of extreme mass ratio (Faulkner, Flannery, & Warner 1972, hereafter FFW). The less massive but more distended component, an evolved object, is transferring material to the primary via an accretion disk, allowing us to view directly the processed by-product of stellar nucleosynthesis and constrain models of stellar nuclear reactions (Marsh & Horne 1991). IBWDs, marking an endpoint of binary evolution, can unravel the history of binary systems, much as solitary white dwarfs represent the end of single-star evolution. Also, the six known IBWDs lie in a temperature range, $\approx$25,000 K (Patterson et al. 1992), where helium is partially ionized and provides an efficient mechanism for driving pulsations (Winget & Fontaine 1982). If we can find even one pulsating white dwarf within a binary system, we can use asteroseismological techniques (Winget et al. 1991) to unlock its structural secrets.

AM CVn (HZ 29, WD 1232+37, PG 1232+379) was discovered by Humason & Zwicky (1947). Its peculiar optical spectrum is characterized by broad, shallow, asymmetric absorption lines of neutral helium and a complete lack of hydrogen (Greenstein & Matthews 1957). Its *IUE* spectrum contains absorption features of Si III, Si IV, C IV, He II, and N IV (Patterson et al. 1992). AM CVn is also a photometric variable, varying its brightness at the 1% level at two independent frequencies; a previously reported double-humped 951.3 μHz (1051.2 s) variation (Smak 1967) and 988.7 μHz (1011.4 s) (Solheim et al. 1984). Flickering, a classic mass transfer signature, is also reported in AM CVn's light curve (Warner &

[1] Department of Astronomy and McDonald Observatory, University of Texas, Austin TX 78712; jlp@chopin.udel.edu.
[2] Department of Physics and Astronomy, University of Delaware, Newark, DE 19716; jlp@chopin.udel.edu.
[3] Guest Observer, Wise Observatory, Israel.
[4] Institutt for Matematiske Realfag, Universitetet i Tromsø, N-9037 Tromsø, Norway.
[5] Department of Physics and Astronomy, Iowa State University, Ames, IA 50211.
[6] Hubble Fellow.
[7] X-2, MS B-220, Los Alamos National Laboratory, Los Alamos, NM 87545.
[8] Guest Observer, Isaac Newton Telescope, Roque do los Muchachos, La Palma, Canary Islands.
[9] Visiting Astronomer, Institute for Astronomy, Honolulu, HI.
[10] Joint Institute for Laboratory Astrophysics, University of Colorado, Box 440, Boulder, CO 80309.
[11] Indian Space Research Organization, Technical Physics Division, ISRO Satellite Center, Airport Road, Bangalore 560 017, India.
[12] Department of Physics and Astronomy, University of Tel Aviv, Ramat Aviv, Tel Aviv 69978, Israel.
[13] Astronomical Observatory of the Institute of Theoretical Physics and Astronomy, Goštauto 12, Vilnius 2600, Lithuania.
[14] Observatoire Midi-Pyrenées, 14 Avenue, E. Belin, 31400 Toulouse, France.
[15] Visiting Astronomer, Canada-France-Hawaii Telescope, operated by the National Research Council of Canada, the Centre National de la Recherche Scientifique de France, and the University of Hawaii.
[16] Observatoire de Paris-Meudon, F-92195 Meudon, Principal Cedex, France.
[17] Physics and Astronomy Department, University of Leicester, Leicester LE1, 7RH, UK.
[18] Steward Observatory, University of Arizona, Tucson, AZ 85721.
[19] Département de Physique, Université de Montréal, C.P. 6128, Succ. A, Montréal, Québec, Canada H3C 3J7.
[20] Instituto de Fisica, Universidade Federal do Rio Grande do Sul, 91501-970 Porto Alegre, RS, Brazil.
[21] Department of Physics and Space Sciences, Florida Institute of Technology, 150 West University Boulevard, Melbourne, FL 32901.
[22] Department of Physics and Astronomy, University of Arkansas, 2801 South University Avenue, Little Rock, AR 72204.

Robinson 1972). No large-magnitude outbursts have been observed.

AM CVn holds the key to unlocking the secrets of IBWDs, but fundamental questions persist. Only circumstantial evidence supports AM CVn's binary nature; we do not see the secondary. The orbital frequency is believed to be 951.3 μHz, but all attempts to find radial velocity variations at this frequency have failed (Lazaro, Solheim, & Arevalo 1989). Despite the 951.3 μHz variation's presumed orbital origin, a predictive ephemeris has never been presented, casting doubt on its frequency and amplitude stability. Solheim et al. (1984) offer a solution with their presentation of Fourier transforms (FTs) in which they find a series of peaks they interpret as pulse-shape harmonics of 951.3 μHz, but no power at 951.3 μHz itself. The authors suggest the true cycle of repeatability is actually 1902.5 μHz (525.6 s). Solheim et al. (1984) also report significant power at 988.7 μHz. If 951.3 μHz is the orbital frequency, we require a second mechanism to produce the 988.7 μHz variation. Finally, Patterson, Halpern, & Shambrook (1993) find line profile variations with a frequency of 20.7 μHz in AM CVn's optical spectra, which they show cannot be the orbital frequency and they interpret as the precession of an elliptical disk.

Our overriding goal in this examination of AM CVn is the precise identification of exactly what frequencies are present in the FTs. We will present the photometric evidence, from FTs, pulse shapes, multicolor photometry, and phase analysis, to choose whether 951.3 or 1902.5 μHz represents the true variations present, whether a stable frequency exists in this system, and which model is best supported by the photometric data.

2. DATA ACQUISITION AND REDUCTION

Our observations consist of 289 hr of white light and multicolor (Johnson *U*, *B*, *V*, and clear) high-speed photometry obtained in 1976, 1978, 1982, 1987, 1988, 1990, and 1992. The contributing sites and telescopes are listed in Table 1.

Nearly half of the data were taken in 1990, during a 2 week Whole Earth Telescope run (Nather et al. 1990). The Whole Earth Telescope (WET), an international collaboration of astronomers around the globe, is designed to obtain 24 hr coverage of a target star, minimizing periodic gaps in the data set. Such gaps introduce alias artifacts into the FT, greatly complicating analysis of multiperiodic variables. We chose AM CVn as a WET target to determine the origin of the multiperiodic photometric variations, to identify additional frequencies, and to search for closely spaced periodicities as an explanation for the inability to create a predictive ephemeris for the 951.3 μHz variation.

All the data were taken with either two- or three-channel photomultiplier-based photometers (Nather 1973), enabling continuous monitoring of a comparison star to verify photometric quality. Observers with two-channel photometers interrupted the light curves at irregular intervals, depending on conditions, to sample sky brightness. When a three-channel photometer was available, the third channel monitored sky brightness, allowing uninterrupted observations of AM CVn. All individual runs employed either 3, 5, 6, or 10 s integration times.

We follow the reduction methods outlined by Nather et al. (1990) to remove sky and extinction effects, producing light curves expressing fractional amplitude relative to mean intensity. We made no attempt to account for different signal-to-noise ratios between individual runs due to telescope aperture, and we did not taper the light curves. An example of a single reduced light curve is given in Figure 1.

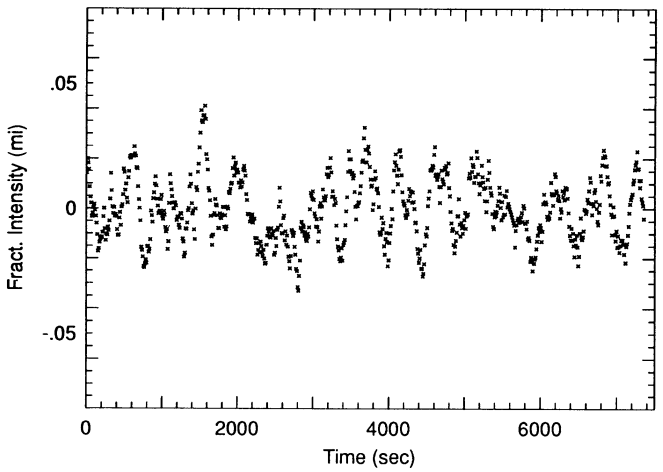

FIG. 1.—AM CVN's light curve obtained with the 3.6 m CFHT. The 1902.5 μHz variation is clearly visible.

Traditionally, we employ the unit "mmg" (millimagnitude) to describe the relative amplitudes of the variations we measure in light curves and FTs (see Winget et al. 1991 for an example). The term "magnitude" implies a logarithmic scale, while we actually measure linear, relative fractional intensities and amplitudes. Therefore, we will adopt the units recently introduced by Winget et al. (1994). Modulation intensity (mi) is a linear representation of fractional intensity of modulation. The modulation intensities we observe in light curves are most conveniently represented in units of mmi (1×10^{-3} mi), where 1 mmi $\approx$ 1 mmg. We will represent our Fourier transforms in units of modulation amplitude (ma) or modulation power [mp = $(\text{ma})^2$], most conveniently in units of mma (1×10^{-3} ma) or μmp (1×10^{-6} mp).

3. OBSERVATIONS

3.1. *Fourier Transforms*

We begin our analysis by examining AM CVn's seasonal power spectra (Fig. 2). The dominant power is consistently at 1902.5 μHz (525.6 s), with additional peaks at 988.7, 2853.8, 3805.2, 4756.5, and 5707.8 μHz (1011.4, 350.4, 262.8, 210.4, and 175.2 s). With the exception of 988.7 μHz, the amplitudes are stable, to within measurement error. We detect no power at 951.3 μHz, the previously reported frequency of variability.

Figure 3 presents a closeup of the 1902.5 μHz region in each seasonal FT. The spectral window, defined as the pattern created in a FT by a single sine wave, of any frequency, sampled exactly as the data, is plotted in each corner. The nearly continuous coverage by WET in 1990, effectively eliminating aliases, reveals additional power at 1923.31 $\pm$ 0.02 μHz (amplitude = 4.4 $\pm$ 0.14 mma), 20.8 μHz from the dominant 1902.5 μHz peak. All other peaks surrounding the 1902.5 μHz peak are artifacts. The combination of power at these two frequencies is consistent with the structure we find in the other seasonal power spectra.

The 2853.8 μHz region contains a triplet, composed of peaks at 2853.8 $\pm$ 0.02, 2874.6 $\pm$ 0.06, and 2895.4 $\pm$ 0.06 μHz (Fig. 4). The average frequency difference between the components, 20.77 $\pm$ 0.05 μHz, is identical to the difference between the 1902.5 μHz doublet. In each example, the "harmonic" peak is the lowest frequency and highest amplitude multiplet member.

TABLE 1

TABLE OF OBSERVATIONS

Run	Telescope	Date	Run Start (UT)	Length (Hrs)	Int (s)
r1722	0.9m Texas	1976 May 27	3:49:54	2.10	5.0
r1724	0.9m Texas	1976 May 28	3:28:44	1.95	5.0
r1727	0.9m Texas	1976 May 29	3:29:00	2.40	5.0
r1730	0.9m Texas	1976 May 30	3:27:32	2.57	5.0
r2093	0.8m Texas	1978 March 8	7:27:00	4.10	10
r2098	0.8m Texas	1978 March 9	5:53:00	5.33	10
r2104	0.8m Texas	1978 March 10	8:38:00	2.43	10
r2106	0.8m Texas	1978 March 11	5:04:00	6.71	10
r2109	0.8m Texas	1978 March 12	3:39:00	6.32	10
r2112	0.8m Texas	1978 March 13	3:22:00	3.18	10
r2123	2.1m Texas	1978 March 17	8:17:50	2.10	3.0
r2126	0.9m Texas	1978 April 1	5:48:00	1.40	5.0
r2130	0.9m Texas	1978 April 3	3:28:20	1.45	5.0
r2131	0.9m Texas	1978 April 3	6:09:20	3.79	5.0
r2137	0.8m Texas	1978 April 11	2:47:00	1.84	5.0
r2138	0.8m Texas	1978 April 11	7:01:00	2.79	5.0
r2141	0.8m Texas	1978 April 12	4:45:00	4.70	5.0
r2146	2.1m Texas	1978 April 13	7:27:31	2.75	5.0
r2149	2.1m Texas	1978 April 15	7:23:00	1.00	5.0
r2151	2.1m Texas	1978 April 17	6:31:16	0.51	5.0
r2156	0.9m Texas	1978 May 7	4:34:20	2.36	5.0
r2163	0.9m Texas	1978 May 9	4:07:40	3.22	5.0
r2170	0.9m Texas	1978 May 12	3:35:20	3.46	5.0
r2190	0.9m Texas	1978 June 5	4:01:20	1.61	5.0
r2205	2.1m Texas	1978 June 8	5:06:57	0.81	5.0
r2352	0.8m Texas	1978 Dec 4	10:13:10	1.05	5.0
r2354	0.8m Texas	1978 Dec 23	9:19:00	3.15	5.0
r2358	0.8m Texas	1978 Dec 24	11:07:30	1.32	5.0
r2362	0.8m Texas	1978 Dec 25	11:29:20	1.04	5.0
r2632	0.9m Texas	1982 Jan 24	9:05:32	3.34	5.0
r2638	0.9m Texas	1982 Jan 27	9:24:08	2.77	6.0
r2641	0.9m Texas	1982 Jan 28	9:08:11	3.37	6.0
r2666	0.8m Texas	1982 May 22	3:16:33	3.27	5.0
r2677	0.9m Texas	1982 June 17	3:33:26	1.36	5.0
run31	0.9m Texas	1987 Feb 2	7:35:00	4.53	5.0
run35	0.9m Texas	1987 Feb 3	7:49:00	4.05	5.0
run36	0.9m Texas	1987 Feb 4	6:30:00	4.65	5.0
run8	0.9m Texas	1987 March 4	5:38:30	2.96	5.0
run26	0.9m Texas	1987 March 5	6:21:40	2.22	5.0
run28	0.9m Texas	1987 March 5	8:52:00	2.98	5.0
run45	0.9m Texas	1987 March 6	6:17:50	2.23	5.0
run47	0.9m Texas	1987 March 6	8:47:50	2.93	5.0
run64	0.9m Texas	1987 March 7	6:14:40	2.23	5.0
run66	0.9m Texas	1987 March 7	8:43:30	2.98	5.0
run68	0.9m Texas	1987 March 8	5:18:10	1.43	5.0
maw-001	0.9m Texas	1988 March 20	2:28:10	1.70	10
maw-004	0.9m Texas	1988 March 21	2:29:20	1.65	10
maw-006	0.9m Texas	1988 March 22	2:26:30	1.66	10
maw-009	0.9m Texas	1988 March 23	2:27:50	1.43	10
maw-0011	0.9m Texas	1988 March 24	2:27:30	1.40	10
maw-0013	0.9m Texas	1988 March 25	2:30:00	1.50	10
maw-0015	0.9m Texas	1988 March 26	2:31:00	4.97	10
pab24	0.8m Texas	1990 March 22	4:57:00	6.69	10
a210	0.6m Hawaii	1990 March 23	7:28:00	7.80	10
ren-0071	1m Israel	1990 March 23	21:49:00	4.86	10
ren-0072	1m Israel	1990 March 24	17:53:30	8.79	10
a212	0.6m Hawaii	1990 March 25	11:39:00	3.38	10
ren-0073	1m Israel	1990 March 25	17:38:00	9.01	10
pab-0029	2.1m Texas	1990 March 26	5:13:30	6.28	10
ren-0074	1m Israel	1990 March 26	17:23:30	9.18	10
a213	0.6m Hawaii	1990 March 27	6:30:00	8.87	10
ren-0075	1m Israel	1990 March 27	17:16:10	9.05	10

TABLE 1—*Continued*

Run	Telescope	Date	Run Start (UT)	Length (Hrs)	Int (s)
a215	0.6m Hawaii	1990 March 28	12:40:00	2.45	10
ren-0077	1m Israel	1990 March 29	00:12:10	2.13	10
en-001	0.9m Texas	1990 March 29	6:01:08	1.60	10
en-002	0.9m Texas	1990 March 29	8:06:44	2.64	10
a217	0.6m Hawaii	1990 March 29	12:56:00	2.23	10
gv-0071	2m OHP	1990 March 30	1:46:57	2.05	10
a220	0.6m Hawaii	1990 March 30	12:56:00	2.09	10
gv-0075	2m OHP	1990 March 31	1:39:40	2.12	10
en-0003	0.9m Texas	1990 March 31	2:29:33	6.60	10
cfc20	0.6m Hawaii	1990 March 31	7:22:20	6.07	10
fbv-002	CFHT 4m	1990 March 31	13:07:57	2.04	10
gv-0079	2m OHP	1990 April 1	6:09:10	1.94	10
cfc23	0.6m Hawaii	1990 April 1	5:35:30	9.05	10
cfc24	0.6m Hawaii	1990 April 2	5:35:30	9.55	10
cfc25	0.6m Hawaii	1990 April 3	5:50:20	4.25	10
jlp-081	0.9m Texas	1992 Jan 14	07:05:33	2.00	5.0
jlp-082	0.9m Texas	1992 Jan 14	09:09:43	3.00	5.0
jlp-084	0.9m Texas	1992 Jan 15	08:07:00	2.94	5.0
jlp-085	0.9m Texas	1992 Jan 15	11:07:50	0.94	5.0
jlp-091	0.9m Texas	1992 April 4	3:11:30	8.37	5.0
jlp-092	0.9m Texas	1992 April 6	8:44:21	2.32	5.0
jlp-093 UBVC	0.9m Texas	1992 April 7	2:54:50	6.50	5.0
jlp-094 UBVC	0.9m Texas	1992 April 9	2:36:10	3.69	5.0
jlp-096	0.9m Texas	1992 May 28	7:42:00	0.93	5.0
jlp-0100	0.9m Texas	1992 June 1	4:46:20	2.52	5.0
jlp-0103	0.9m Texas	1992 June 3	3:56:00	2.13	5.0
jlp-0104	0.9m Texas	1992 June 3	6:07:30	0.54	5.0
jlp-0105	0.9m Texas	1992 June 3	6:46:20	0.48	5.0

Unlike the other significant peaks, the 988.7 μHz peak's amplitude is variable. Power is nearly absent in 1982 and 1990, but is almost equivalent to the 1902.5 μHz power in 1987 and has an intermediate amplitude in 1988. However, the frequency does not vary outside measurement errors.

Thanks to the improved signal-to-noise ratio provided by WET, we uncovered additional low-amplitude power near 654 and 1249 μHz in several of our seasonal FTs. These peaks are numerically related to but not integer multiples of 951.3 μHz. We also find a low-amplitude peak at 972.03 ± 0.05 μHz (1028.78 s) in the 1990 FT, which we point out because it is 20.7 μHz from 951.3 μHz, the same frequency difference observed within the 1902.5 and 2853.8 μHz multiplets. We do not find evidence for additional stable periodicities, although other significant peaks are occasionally present in individual FTs. These short-lifetime, nonrepeating variations could be related to the reports of flickering in AM CVn.

3.2. *Pulse Shapes*

A pulse shape is an average waveform constructed by folding a light curve at a period of interest. Noncommensurate frequencies will not have a significant effect on the pulse shape if the data cover a time base greater than the inverse frequency difference of the closest periodicities (Bracewell 1965). Pulse shapes contain the same information as FTs, but provide a complementary way to interpret the harmonic structure associated with a variation. Harmonics in a FT may arise in two ways: a nonsinusoidal variation will produce "pulse shape" harmonics, or the harmonics may represent independent periodicities in their own right.

The 1902.5 μHz seasonal pulse shape (Fig. 5) is remarkably stable in amplitude and profile. We also constructed pulse shapes for the 988.7 μHz variation, when it was present in the FT (Fig. 6). It does not maintain a stable shape, in contrast to the 1902.5 μHz variation. Different mechanisms are clearly responsible for the two variations.

3.3. *Simultaneous Multicolor Photometry*

Several of our individual AM CVn light curves are multicolor (*UBV* and clear) observations, acquired by rotating a set of Johnson *U*, *B*, and *V* filters and one clear aperture through the light beam. We obtained these observations to study the photometric variations as a function of color, with interesting results (Fig. 7). The 988.7 μHz peak has its largest amplitude in the *V* band (5.8 ± 0.4 mma vs. 3.3 ± 0.6 [*B*] and 4.8 ± 0.6 [*U*]), suggesting an origin in AM CVn's cooler regions. The power at 1249 μHz and an unexplained peak at $\approx$1600 μHz are strongest in *U*, suggesting an origin in hotter parts of the system.

The 1902.5 μHz average pulse shapes for each color have the same amplitude, phase and general shape (Fig. 8). This color-independence suggests that we are observing a variation arising within a hot region of AM CVn. Since high-temperature blackbody curves are nearly parallel in the *UBV* region, we would expect little amplitude change with color.

4. 951.3 OR 1902.5 μHz?

4.1. *The Case against* 951.3 μHz *as the Photometric Frequency*

One of our goals in this investigation is a solution to the 951.3 versus 1902.5 μHz frequency of repeatability debate begun by Solheim et al. (1984). Nonsinusoidal waveforms exist which the FT process will translate into a series of pulse-shape harmonics of the true period of repeatability (Fig. 9). At first

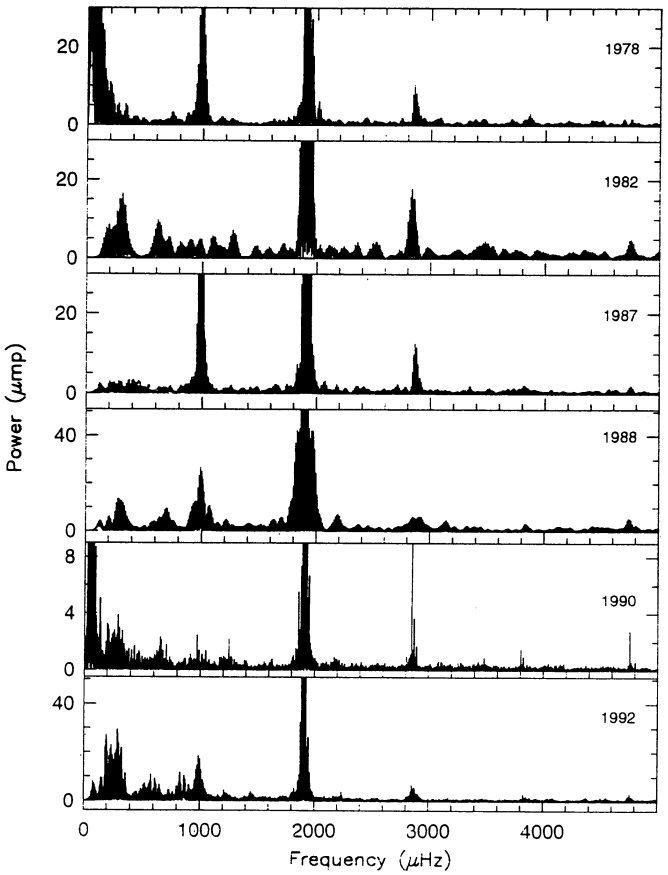

FIG. 2.—Seasonal Fourier transforms of AM CVn. The dominant power is at 1902.5, 2853.8, 3805.2, 4756.5, 5707.8, and 988.7 μHz (525.6, 350.4, 262.8, 210.2, 175.2, and 1011.4 s). Note the changes in each panel's vertical scale, to span the dynamic range present.

glance, the presence of an exact harmonic series of 951.3 μHz in AM CVn's FTs suggests this as the frequency of the system. Unfortunately, the situation is not so simple. A harmonic is defined as (Bracewell 1965)

$$H_n = n\nu_0 \quad (1)$$

where H and ν_0 are frequencies and n is an integer. The 1902.5 and 2853.8 μHz peaks are multiplets, comprised of up to three individual peaks separated by 20.77 μHz. While complex structure of pulse-shape harmonics is possible, the frequency splitting in each should increase as the harmonic number increases. The constant 20.77 μHz fine structure observed in AM CVn is not consistent with the simple pulse-shape hypothesis. We also cannot easily explain why some and not all the harmonics exhibit fine structure.

The 654 and 1249 μHz power strike an additional blow to the hypothesis of simple harmonics of an unseen fundamental frequency. These peaks are numerically related to, but not integer multiples of, 951.3 μHz, and so cannot be pulse-shape distortions. We conclude that the numerically related peaks in the power spectra are not simple harmonics of 951.3 μHz but must arise via more complex mechanisms.

4.2. *The Case for* 1902.5 μHz *as the Photometric Frequency*

As an alternative, we propose that AM CVn contains at least two independent frequencies, 988.7 and 1902.5 μHz. We have found six main frequencies in AM CVn's power spectra: 988.7, 1902.5, 2853.8, 3805.2, 4756.5, and 5707.8 μHz, as well as the associated 20.77 μHz structure. Because of its amplitude variability, average pulse shape, and color characteristics, it is fair to argue that the 988.7 μHz peak and the five numerically related frequencies have different origins. We designate 988.7 μHz as ν_1 and turn our attention to the five remaining frequencies. Since 1902.5 μHz has the largest amplitude, we designate it as ν_0. The 3805.2 and 5707.8 μHz peaks become $2\nu_0$ and $3\nu_0$, the first and second harmonics of ν_0.

We next focus on the 2853.8 μHz multiplet, consisting of a triplet with 20.77 μHz splitting and stable amplitudes. Because the frequency difference is identical to the 1902.5 μHz doublet, we designate the 2853.8 μHz power as a second variation, ν_0^1. We use ν_0^1 because this peak is numerically related to 1902.5 μHz and may be driven by the same mechanism, and hence not truly independent. The same basic argument applies to the low-amplitude 1249 μHz power, which we designate ν_0^2, although we cannot comment conclusively on its amplitude stability or the presence of fine structure.

One additional frequency, at 4756.5 μHz, remains. This peak is not a harmonic of either 1902.5 or 2853.8 μHz and has no associated complex structure. Its frequency, however, is the sum of 1902.5 and 2853.8 μHz, so this peak may be a linear combination. We find two additional linear combinations,

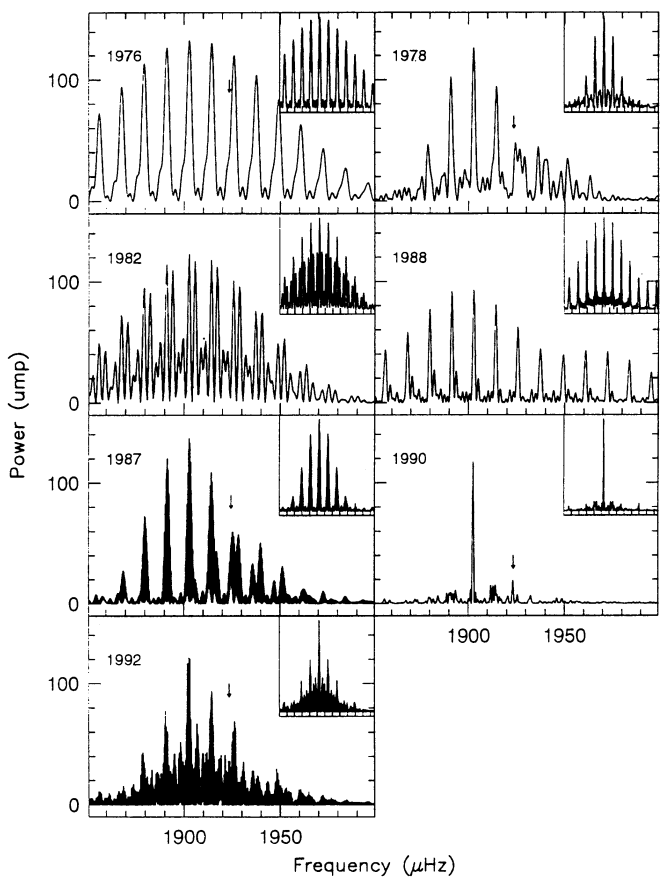

FIG. 3.—The 1902.5 μHz region of AM CVn's FT in each season. The spectral window, the pattern generated by a single sinusoid sampled exactly as the original data, is given, on a slightly different frequency scale, in the upper right-hand corner of each FT. The arrow marks the location of the 1923.3 μHz peak.

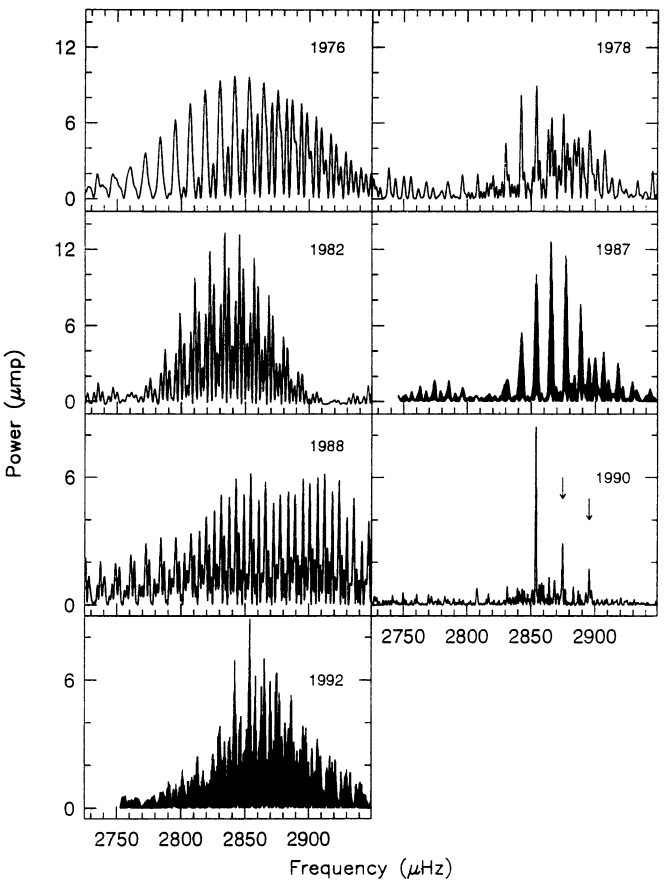

FIG. 4.—The 2853.8 μHz region in each season's FT of AM CVn. Each window spectrum is given in Fig. 3. Each season's FT is consistent with the presence of the triplet clearly resolved in 1990.

1902.5 + 1923.3 = 3825.8 μHz, and 1902.5 − 1249 = 654 μHz. The 1902.5, not 951.3, μHz peak is always involved in the combinations, again indicating its reality.

As an alternative to a pulse-shape harmonic series, we can account for all of AM CVn's frequencies in terms of one completely independent variation, three numerically related frequencies probably arising from the same mechanism, and their accompanying harmonics and linear combinations.

5. PHASE STABILITY

Since AM CVn's discovery, controversy has surrounded the phase stability of its photometric variations. Numerous authors have presented ephemerides and found the supposed 951.3 μHz variation to be increasing rapidly ($P = +3.8 \times 10^{-10}$ s s^{-1}; Patterson, Nather, & Robinson 1979), decreasing [$\dot{P} = (-3.2 \pm 0.6) \times 10^{-12}$ s s^{-1}; Solheim et al. 1984], and incoherent (Patterson et al. 1992). A predictive ephemeris has never been published. AM CVn has also been reported to exhibit "phase jitter," in which the phase of the dominant variation wanders by as much as a quarter of a cycle on timescales of days (Warner & Robinson 1972).

The traditional method of phase analysis is the $O-C$ diagram, a series of points characterizing a variation's behavior relative to an ephemeris (Kepler et al. 1991). An accurate model for a stable frequency will produce a set of $O-C$ points best fitted by a straight line with zero slope.

Previous $O-C$ diagrams for AM CVn use timings obtained from a single night of observations (Solheim et al. 1984). Unfortunately, the 1902.5 μHz doublet requires 13.4 hr of continuous data to resolve, so a timing from a single night will not be accurate. Combining light curves from successive nights of single-site observations introduces overlapping alias patterns. In AM CVn's case, even two nights of observations are not satisfactory; the FT must contain a sufficient time base to resolve the web of aliases. To illustrate, the 1987 FT (Fig. 3) demonstrates the significance of the overlapping alias patterns from the small 1923.3 μHz peak. If the FT's resolution were reduced, the aliases from the small component would contribute significantly to the power in the dominant peak. The measured timing could be "pulled" by as much as ±80 s.

We will minimize these problems by calculating seasonal timings for the 1902.5 μHz frequency to ensure complete resolution of the power spectra. Before we can perform this analysis, and considering AM CVn's history, we must show the 1902.5 μHz peak to be stable in both frequency and amplitude to eliminate the possibility of two or more unresolved variations beating together (Winget et al. 1991). The 1902.5 μHz variation does exhibit the same frequency and amplitude, within measurement errors, in every adequately resolved FT available (Table 2).

Next, we must determine the peak's frequency to sufficient accuracy to avoid cycle count ambiguities over unavoidable gaps in the data set. The best seasonal frequency, from 1992, is 1902.522 ± 0.001 μHz, accurate enough to determine timings for a stable variation for over 3 years before losing one-tenth of

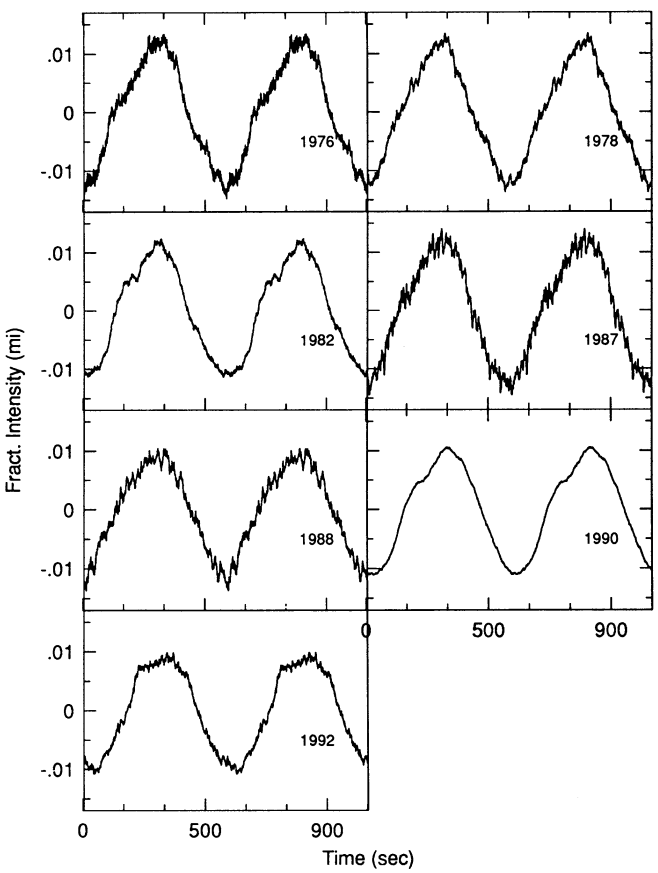

FIG. 5.—The 1902.5 μHz seasonal pulse shapes. The amplitudes and general profiles of all pulses are nearly identical.

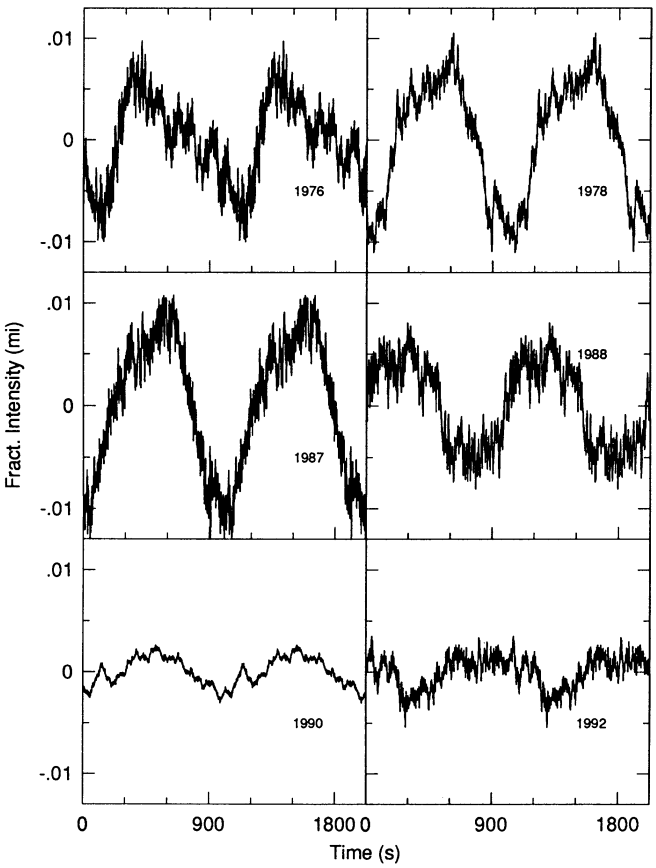

FIG. 6.—The 988.7 μHz seasonal pulse shapes. The amplitudes and profiles vary greatly, in contrast to the behavior of the 1902.5 μHz pulse.

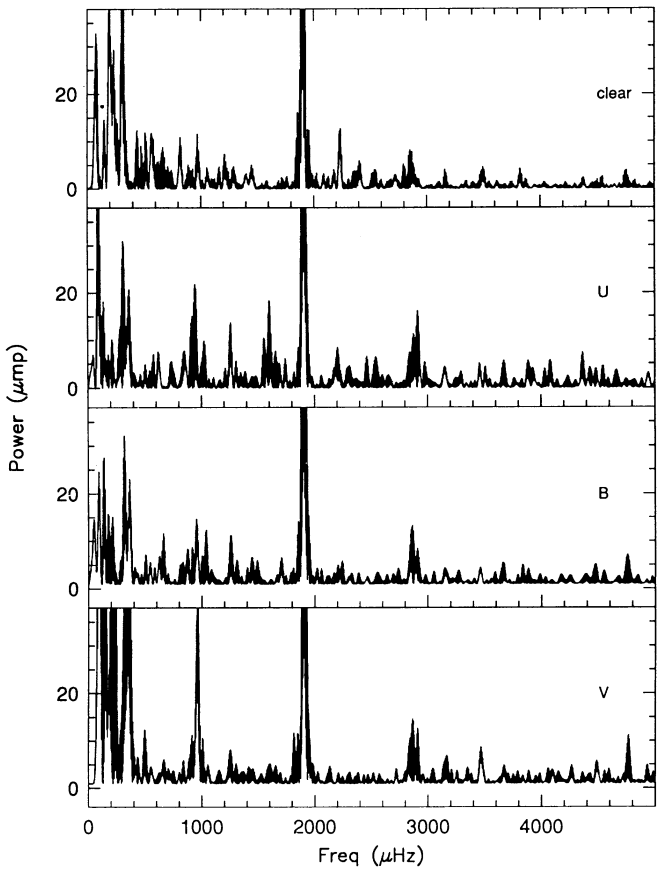

FIG. 7.—Multicolor *UBV* and clear photometry of AM CVn. Power with different amplitudes in different colors may be occurring in different temperature regions of the system.

a cycle. This value is consistent with the 1990 seasonal frequency, so we can combine these two seasons to improve our knowledge of the frequency. The best frequency for 1990–1992 is 1902.5115 $\pm$ 0.0001 μHz. If we continue in this manner, making sure the amplitude remains stable, we end up with a best value for the entire data set of 1902.509804 $\pm$ 0.000003 μHz.

If the 1902.5 μHz variation is strictly coherent, we expect the measured seasonal frequencies (Table 2) to agree with our best value for the entire data set. The data set value is about 1 σ from the 1990 frequency, but is nearly 5 σ from the 1978 frequency and 11 σ from the 1992 value. A strictly coherent model is not adequate for AM CVn; we must incorporate some type of period change.

We begin by examining the stability of the 1902.5 μHz variation over short timescales and placing a limit on its rate of period change. Figure 10 is the $O-C$ diagram for the best period from the 1990 WET data set, 1902.517 $\pm$ 0.02 μHz. The scatter is about 15 s, consistent with our ability to measure the actual time of minimum (or maximum) of a variation within a light curve. Although WET was only 10 days long, we can place an upper limit of $\dot{P} < +2.3(\pm 1.4) \times 10^{-8}$ s s^{-1}. We can

TABLE 2

SEASONAL FREQUENCIES FOR AM CVn

Year	Frequency (μHz)	Uncertainty (μHz)	Amp (mma)	Uncertainty (mma)
1992	1902.522	0.001	11.7	0.2
1990	1902.52	0.02	10.5	0.3
1988	1902.72	0.05	9.6	0.3
1987	1902.53	0.03	11.4	0.2
1982	1902.55	0.04	11.3	0.5
1978	1902.66	0.03	11.4	0.3
90 – 92	1902.511470	0.000069	11.11	0.18
88 – 92	1902.512020	0.000043	10.61	0.14
87 – 92	1902.509820	0.000027	11.18	0.14
82 – 92	1902.510110	0.000021	10.42	0.14
78 – 92	1902.509802	0.000010	10.51	0.11

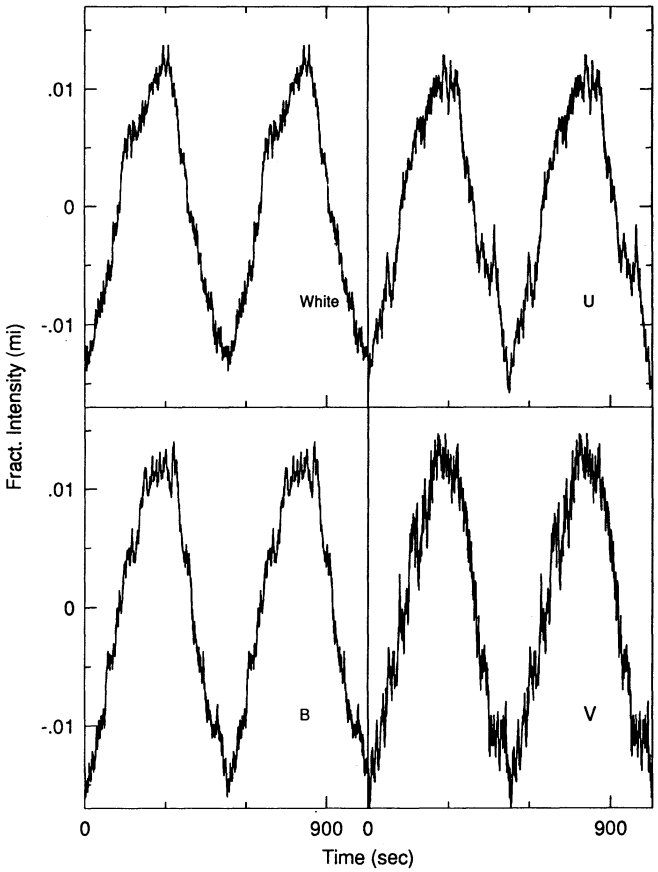

FIG. 8.—Dominant 1902.5 μHz average pulse shape in each color band. The amplitudes and phases are independent of color.

also eliminate the possibility of any rapid, random phase changes on timescales of days.

Next, we use the 1992 season to test the stability over a timescale of months. Table 3 lists the $O-C$ timings for 1992 April and June, demonstrating the stability of the 1902.5 μHz variation over this timescale.

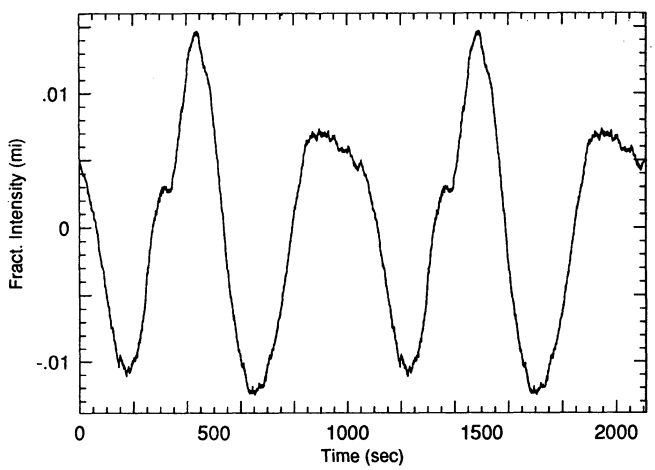

FIG. 9.—The 951.3 μHz pulse shape from the 1990 data. This pulse shape can be created by an interaction between the 1902.5 and 2853.8 μHz peaks. There is a slight difference in the depths of the two minima, but this would be indistinguishable in a single night of observation.

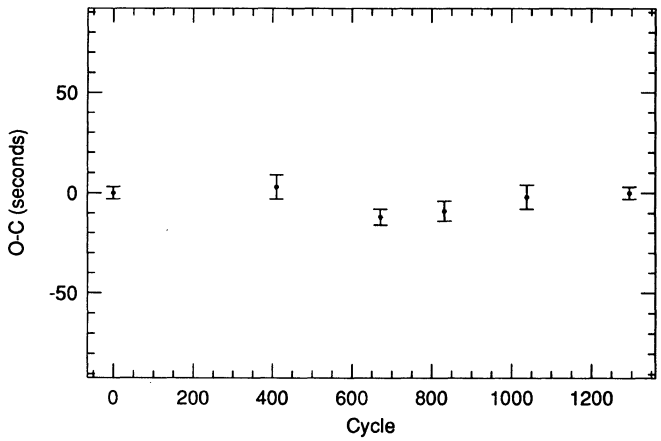

FIG. 10.—$O-C$ diagram for the 1990 WET observing run. We can place a limit of $|\dot{P}| < +2.3(\pm 1.4) \times 10^{-8}$ s s^{-1} for the 1902.5 μHz variation.

We can improve our $\dot{P}$ limit by examining the change in the best frequencies for each season (Table 2) and limiting the period change via $\dot{P} < (\Delta P/\Delta T)$, where $\Delta P = (1/f_2) - (1/f_1)$. Using the 1990 and 1992 frequencies, $|\dot{P}| < +2 \times 10^{-10}$ s s^{-1}; otherwise we would see a greater change in the seasonal frequencies. This figure is consistent with the difference between any two seasons, and is comfortably below our earlier limit.

To calculate our $O-C$ points, we fitted a 1902.509804 μHz sinusoid to each observing season's data. Because the 1992 season spans the longest time base, we designate this season's T_{max} as T_{zero}, and give it an $O-C$ value of 0 s. We reference all other $O-C$ points to this initial timing.

Our constrained, but nonzero, value of $\dot{P}$ will introduce cycle-count aliases between observing seasons, greatly increasing the possible solutions to the $O-C$ diagram. From 1990 to 1992, we could accumulate ± 1 cycles, eliminating solutions that in 1990 pass through cycle-count aliases greater than this. Applying similar limits to other $O-C$ points results in the fan-shaped plot in Figure 11. In order to prove that we measure a period change, all possible solutions except one must be eliminated to a high degree of confidence.

We calculated fits for values of constant $\dot{P}$ by fitting (Kepler et al. 1991)

$$(O-C) = T_{max}^{obs} - T_{zero} - PE - \tfrac{1}{2}P\dot{P}E^2 , \qquad (2)$$

where E is the number of cycles which elapse until T_{zero} and $P = 1/f = 525.621470$ s, to the points in the $O-C$ diagram. We examined all possible solutions, including linear ones, to the values from 1992, 1990, 1987, and 1982, and tested each fit's predictive ability by then including the 1978 and 1988 points. In most cases, the fit failed this test by changing by at least 10 σ, allowing us to eliminate those potential solutions based on lack of predictive ability. The only fit exhibiting predictive power by changing by less than 1 σ is $\dot{P} = +1.68(\pm 0.03) \times 10^{-11}$ s s^{-1} (Fig. 12). In this case, the $O-C$ points lie within 3 σ of the fitted parabola (Table 4). The probability of obtaining six random points that lie on a parabola is 1 in 125,000.

To confirm this value for the period change, we fitted a sinusoid with various values of $\dot{P}$ to the entire data set. The best value for $\dot{P}$ obtained via this method is $+1.73(\pm 0.03) \times 10^{-11}$ s s^{-1}, in agreement with that obtained directly from the $O-C$ diagram. Our measured rate of period change is therefore $+1.71(\pm 0.04) \times 10^{-11}$ s s^{-1}, correspond-

TABLE 3

$O-C$ TIMINGS

Date	T_{max} (s)	Start BJED	Offset (s)	E	O-C (s)
1992 April	375 ± 2	8635.798648	6984620	0	0 ± 2
1992 June	184 ± 2	8635.798648	11873060	9300.002	1 ± 2

NOTE.—T_{max} is the observed time of maximum, "Start" is the barycentric Julian ephemeris date to which the data are referenced, and E is the number of cycles elapsed between T_{max} and T_{zero}.

ing to a timescale of

$$\frac{P}{\dot{P}} \approx 1 \times 10^6 \text{ yr} . \quad (3)$$

6. THE PHYSICAL NATURE OF AM CANUM VENATICORUM

AM CVn is a complex, confusing object. Our analysis of this extensive data set has pinpointed facts a satisfactory model of the object must explain: (1) AM CVn is multiperiodic, with at least two independent variations, at 1902.5 and 988.7 μHz; (2) there is a lack of power at 951.3 and 20.77 μHz fine structure associated with only two "harmonics"; (3) the 1902.5 μHz power is stable in amplitude, while the 988.7 μHz variation is not; (4) the 1902.5 μHz power's amplitude and phase are color-independent, while the 988.7 μHz peak is largest in V; (5) the nonsinusoidal 1902.5 μHz pulse is stable in shape; (6) the 988.7 μHz power has a variable pulse shape; (7) our measurement of $\dot{P} = +1.71 \times 10^{-11}$ s s^{-1} for the 1902.5 μHz second frequency is a strong indication of its long-term stability; and (8) the numerical relationship between 1902.5 and 2853.8 μHz, their constant amplitudes, and the presence of identical 20.77 μHz splitting suggest that these two periodicities have a common physical origin.

The corpses of unburied models litter AM CVn's wake. In our quest to clear up the confusion, we will sift through the observational facts to determine which direction the data force us to travel to explain AM CVn. We will begin with models incorporating single stars, the simplest possible starting position, and ask (1) what phenomena the model predicts and (2) whether the model can explain AM CVn's observed behavior.

6.1. *Single-Star Models*

We can immediately eliminate all single-star models which cannot produce two unrelated frequencies, such as a magnetic rotator. We can also eliminate a helium white dwarf analog of the rapidly oscillating Ap stars (Kurtz, Shibahasi, & Goode 1990). AM CVn does not exhibit the 180° phase changes predicted by this model.

The simplest multiperiodic single-star model is a DB pulsator (DBV). The general features of DBVs—a lack of hydrogen, a range of possible periods of pulsation from ≈100 to 1000 s, a large number of modes simultaneously excited in an individual star, and an effective temperature of ≈25,000 K (Unno et al. 1989)—agree well with AM CVn's characteristics.

In many ways, AM CVn resembles PG 1351+498, a well-studied DBV (Winget, Nather, & Hill 1987). If the 1902.5 μHz

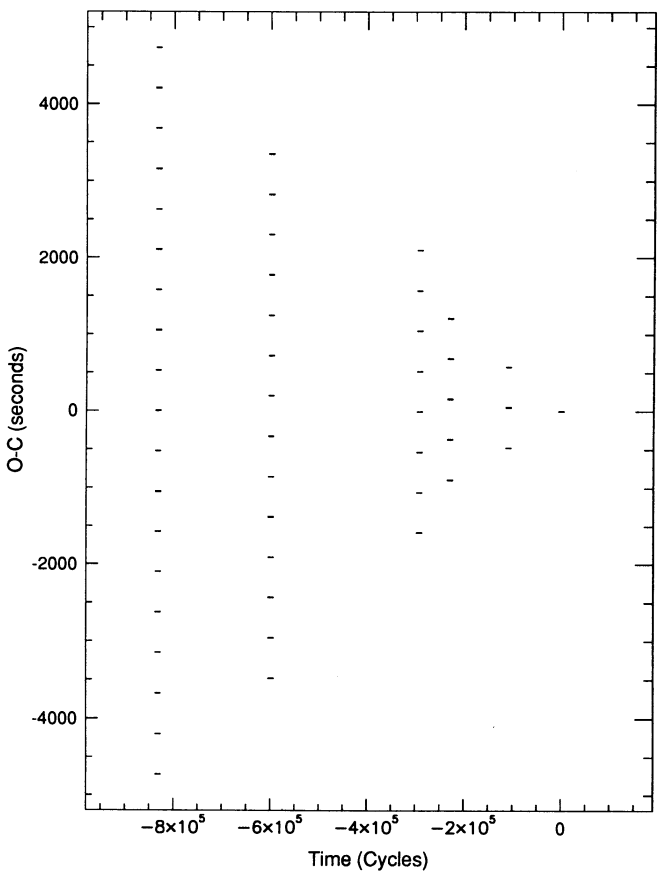

FIG. 11.—$O-C$ diagram for AM CVn's 1902.5 μHz variation, representing all possible timings given our limit on the rate of period change. A solution must pass through one timing from each season.

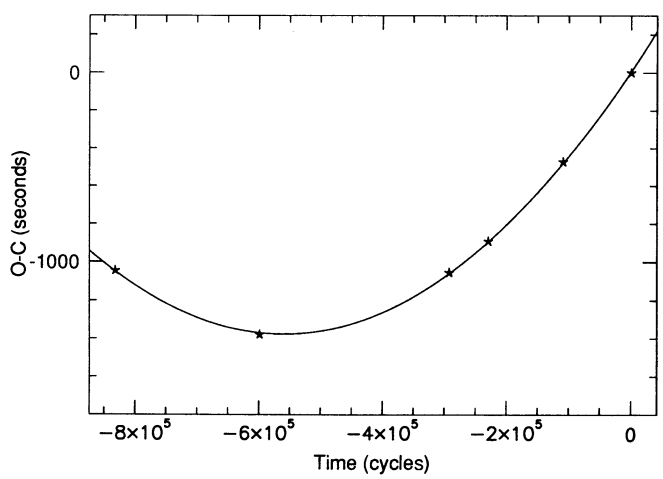

FIG. 12.—Best fit to the $O-C$ points in Fig. 11. The 1 σ uncertainties are represented by the size of the points.

TABLE 4

$O-C$ FOR 1902.509802 μHz

Cycle	O-C (s)	Δ Fit (s)	Uncertainty (s)
0	0	-6.5	2
-108996	-472.6	6.2	2
-229337	-891.0	2.1	3
-292107	-1055.2	3.4	1
-598647	-1378.1	-9.4	3
-831744	-1046.2	4.2	2

NOTE.—Comparisons of $O-C$ timings with values from our best fit. Δ Fit is the difference between the timings and the fit. The uncertainties are 1 σ timing errors.

peak is ν_0, AM CVn's power spectrum has power at $(2/3)\nu_0$, $(2/2)\nu_0$, $(3/2)\nu_0$, $(4/2)\nu_0$, $(5/2)\nu_0$, and $(6/2)\nu_0$, similar to the pattern found in the DBV PG 1351+498. However, the numerical relations we find for PG 1351+498 are not exact fractions but are rather 1.47, 2.47, etc. The relative amplitudes of the various frequencies also differ.

Fine structure associated with each mode is a characteristic of nonradial pulsators. From a theoretical perspective, nonradial pulsations are described in terms of spherical harmonics represented by the harmonic index l, the radial overtone number k, and the azimuthal quantum number m. Rotation destroys the star's spherical symmetry, lifting the m degeneracy, and splitting each mode into $2l+1$ separate frequencies. In the limit of slow rotation and large values of k, the frequency difference between m's measures the rotation frequency of the star (Unno et al. 1989). Observed frequency splittings range from 4.2 μHz ($l=1$) for the DOV pulsator PG 1159 (Winget et al. 1991) to 6.5 μHz ($l=1$) for the DBV GD 358 (Winget et al. 1994), corresponding to rotation periods of 1.38 and 0.89 days, respectively. If AM CVn is a DB pulsator, and we identify the 1902.5 and 2853.8 μHz peaks as $l=1$ modes, the star's rotation period is 6.7 hr, a factor of 5 or so shorter that that of GD 358 (Winget et al. 1994).

Sum and difference frequencies are also found in the power spectra of all large-amplitude pulsators (Winget et al. 1994). These combination frequencies are consistent with pulse-shape effects arising from the pulsation's nonlinear nature (Winget et al. 1994). We find three possible linear combination frequencies in AM CVn's power spectra, at 4756.5 μHz = 1902.5+2853.8 μHz, 3825.8 μHz = 1902.5+1923.3 μHz, and 654 μHz = 1902.5−1248.8 μHz. We could also interpret the small peak at 972.0 μHz mentioned earlier as the frequency difference between 1902.5 and 2874.55 μHz.

This is very promising, but the single DB pulsator model has several flaws. Most important, AM CVn's optical and *IUE* spectra are very different from, and cannot be explained as, those of a typical DB white dwarf (Patterson et al. 1992). Second, the luminosity variations of pulsating white dwarfs are a manifestation of temperature changes on the stellar surface (see Provencal 1993 for examples). It is difficult to imagine how a temperature change could create AM CVn's asymmetric pulse shape. Finally, the predicted value of $\dot{P}$ due to evolutionary cooling of a 25,000 K DB pulsator is $\approx 5\times10^{-14}$ s s^{-1} (Bradley 1993), over 300 times smaller than our measurement. While this does not invalidate the DB model, if AM CVn is indeed a DB pulsator, the period change cannot result from white dwarf evolutionary cooling.

6.2. *Binary Systems*

We find a DB pulsator an unsatisfactory model for AM CVn, forcing us to consider binaries. Binary systems come in many colors and flavors, but we can restrict the possible components. Hydrogen's absence in AM CVn's spectrum eliminates all binary models harboring a low-mass main-sequence star (FFW). We also dismiss a helium-burning main-sequence star, as all evidence indicates that AM CVn is faint and relatively nearby (Solheim et al. 1984). If we assume that the photometric variations represent the orbital frequency, the nondetection of radial velocity variations in the helium absorption lines for frequencies of 1902.5, 988.7, 494.4, and 951.3 μHz (Lazaro et al. 1989) suggests a low-mass companion. If the orbital frequency corresponds to either 1902.5 or 988.7 μHz, and the accretor has a mass of 1 $M_\odot$, the secondary must be a helium white dwarf between 0.02 and 0.04 $M_\odot$ (FFW).

We can immediately eliminate a simple interacting twin degenerate system. Although AM CVn's optical and *IUE* spectra are consistent with this model (Patterson et al. 1992), it cannot produce multiple frequencies. We must create at least two frequencies but have only one orbital period.

Our next step is to include a magnetic field. AM CVn is not a strong X-ray source (Becker 1981), but it has been detected by *ROSAT* (Solheim 1994). There is no evidence of circular polarization (Angel & Landstreet 1970; Solheim 1989), but current techniques can detect magnetic fields only down to about 10^6 G. Although we have no compelling evidence arguing for a magnetic field in AM CVn, we can find no evidence against a field as great as 10^6 G.

A magnetic field of 10^5–10^6 G would have interesting effects on AM CVn's structure. If we assume the accretor's rotation timescale to be shorter than the binary period, we designate 988.7 μHz as the orbital frequency of the system, and 1902.5 μHz as the rotational frequency of the white dwarf. Assuming $M_1 = 1\ M_\odot$ and $M_2 = 0.04\ M_\odot$ (FFW), from Kepler's law we get a separation of $a \approx 1.5\times10^{10}$ cm. We use equations for the case of extreme mass ratio given by Frank, King, & Raine (1985) to calculate Roche lobe dimensions of $R_{L,2} = 0.16a = 2.4\times10^9$ cm and $R_{L,1} = 0.84a = 1.3\times10^{10}$ cm. The circularization radius, a lower limit on the size of the accretion disk, is 7.0×10^9 cm (Frank et al. 1985).

The magnetospheric radius of the accretor is dependent on the magnetic field strength, the mass of the accretor, and the accretion rate. We assume an accretor mass of 1 $M_\odot$, a magnetic field ranging from 10^5 to 10^6 G, and an accretion rate of $1\times10^{-10}\ M_\odot$ yr^{-1} (Solheim et al. 1984). We use equations given in Frank et al. (1985) to determine a range for the radius for stream accretion, $R_{\rm mag}$, from 1.9×10^9 to 7.0×10^9 cm. These values of $R_{\rm mag}$ lie within the circularization radius but above the white dwarf's surface ($R \approx 6\times10^8$ cm). If such a magnetic field is present, AM CVn could be a helium version of an intermediate polar (Warner 1986).

Patterson et al. (1993) found the helium lines in AM CVn's optical spectrum to undergo profile variations at $\approx$20.7 μHz, which they interpret as precession of an elliptical disk. We can advance an alternative explanation for the absorption profile variations. Following the intermediate polar model, the material accreting onto the white dwarf's magnetic poles must create a torque, forcing the white dwarf to precess. The absorption features originate in the accretion disk, but are partially

filled with emission emanating from the hot poles. As the poles precess at 20.77 μHz, the emission profiles vary, appearing to modulate the absorption features. We can explain the differences in phase of the profile variation in the core of the absorption lines and in the wing regions (Patterson et al. 1993) as reprocessing of the beam as it sweeps across the disk.

Hirose & Osaki (1990) calculated theoretical models of accretion disks within systems of extreme mass ratio. They find that such disks become unstable and precess, and predict a beat frequency between the orbital and precession frequency, for a system similar to AM CVn, of 20 μHz, close to our observed 20.77 μHz fine structure. However, there is no theoretical reason why the precession period should remain stable for more than the viscous timescale of the disk (Zhang et al. 1991). The SU UMa stars are another class of interacting variables believed to contain precessing ellipticl disks. During a SU UMa outburst, $\dot{P} \approx 5 \times 10^{-5}$ s s^{-1}, corresponding to a viscous timescale of a few weeks. We detect the 20.77 μHz structure in a number of AM CVn's seasonal FTs, indicating a timescale measured in years, not weeks. Also, the optical light from the system should be modulated as the aspect angle of the disk changes with the precession period (Meyer & Meyer-Hoffmeister 1984). We find no variations at 20.77 μHz in our photometric data, to a limit of 3 mma, arguing against even a modestly asymmetric disk.

The helium intermediate polar model has difficulty explaining some of AM CVn's characteristics. If 1902.5 μHz represents the accretor's rotational frequency, we should measure a negative $\dot{P}$-value as the white dwarf accumulates angular momentum from the accreting material. However, in a magnetic system, $\dot{P}$ represents a convolution of magnetic braking and accretion. If the field is strong enough to couple to the outer disk, magnetic braking could transfer momentum back outward, tending to increase rather than decrease the rotation period. Second, the 2853.8 μHz power and its harmonics are difficult to explain, unless we assume we are viewing two poles of unequal brightness. The white dwarf's rotation frequency would then be 951.3 μHz, longer than the orbital timescale. And, finally, intermediate polars display linear combinations of the orbital and spin periods (Warner 1986). However, we cannot explain AM CVn's combination in terms of orbital and spin frequencies. The observed sum and difference frequencies are combinations of 1902.5 μHz with *three different* frequencies.

Our final binary model contains a DB pulsating white dwarf, embedded in an accretion disk, as a member of an interacting binary. The temperature of the systems is commensurate with known DBVs, the periods of the variations are within the expected range, and the amplitudes are similar to those observed in solitary pulsators, especially when considering a DB pulsator viewed against the background of a bright accretion disk. The optical and *IUE* spectra would combine characteristics of an accretion disk and a white dwarf.

Combining the factors in favor of the single DBV model with those of a simple accretor can explain all the behaviors of AM CVn. However, there is one fatal flaw with the DB pulsating accretor model. The rotation period of 6.7 hr derived from the frequency splitting is much slower than the presumed orbital period of the binary. The 20.77 μHz fine structure cannot be rotational splitting. As an alternative, we can modify our assumptions for an intermediate polar and interpret the 20.77 μHz structure as a precession of the pulsation axis in response to the torque produced by accreting material.

If 1902.5 μHz represents a nonradial pulsation on an accreting white dwarf, the interpretation of $\dot{P}$ is ambiguous. Our hypothetical white dwarf pulsator in AM CVn is anything but a typical pulsator, and its outer layers are certainly not cooling, but are being heated to a depth dependent on the accretion timescale. The accretor's thermal structure would be very bizarre, with a hot envelope surrounding a cooler core indicative of the primary's original temperature when the current accretion episode began. The accreting pulsator's rate of period change will be modified by the balance between heating the outer layers and core cooling. We need a theoretical framework of appropriate white dwarf models to investigate how the rate of period change is affected by accretion.

To end our discussion of binary models, we must mention an important component of AM CVn: the mass-losing secondary. The accretion disk probes the secondary's composition, and, by extension, the composition of what was once a main-sequence star's core. Surprisingly, the secondary seems to be composed solely of helium, with a smattering of other heavy metals. At 0.04 $M_\odot$ we should be well into the carbon core if this star followed a normal evolutionary track. A single main-sequence star without enough mass to burn helium to carbon has not had sufficient time to evolve to a white dwarf. The secondary must have been deprived of a normal main-sequence lifetime because of its membership in the binary. Such a star's dynamical timescale is several hundred seconds (Unno et al. 1989), corresponding to the timescale of the variations seen in AM CVn. If the secondary has radial pulsations excited, it could modulate mass transfer at these rates.

7. SUMMARY AND CONCLUSIONS

AM CVn's FT contains power at 988.7, 1248.8, 1902.5, 2853.8, 3805.2, 4752.9, and 5707.8 μHz. In contrast to the previous interpretation of these frequencies as simple pulse-shape harmonics of an unseen fundamental, we believe these periodicities can be better explained by one completely independent frequency and three numerically related frequencies probably driven by the same mechanism, with two harmonics and linear combinations. Our most important results are (1) that past interpretation of AM CVn's FT as a harmonic series of an unseen fundamental 951.3 μHz frequency is too simplistic, and (2) that the 1902.5 μHz frequency's long-term coherence, with $\dot{P} = +1.7 \times 10^{-11}$ s s^{-1}.

Despite our wealth of observational data, AM CVn remains mysterious. We confirm the likelihood that AM CVn is a s binary, but we cannot explain its photometric behavior as a simple interacting binary, or as an interacting system containing a precessing accretion disk as proposed by Patterson et al. (1993). An intermediate-polar model fits most of the observations, but has problems. Our best model contains a pulsating DB embedded within the system. This model can explain all of the photometric behavior of AM CVn, if the 20.77 μHz structure is not due to rotation. The role of pulsation in this system cannot be discounted.

Our work hinges on the assumption that one of the photometric variations represents the orbital frequency, but we have no conclusive evidence of the orbital variations. Profile changes with a 20.7 μHz frequency have been detected in AM CVn's spectra but cannot be orbital in origin (Patterson et al. 1993). If 988.7 μHz is the orbital frequency, it should maintain a stable phase, but its amplitude variations will make an ephemeris calculation difficult. We are hopeful because the 988.7 μHz variation appears to maintain frequency. The 2853.8

μHz power's phase stability must also be investigated. If both the 1902.5 and 2853.8 μHz frequencies are driven by the same mechanism, they should be affected on the same timescale. Therefore, we predict $P/\dot{P} \approx 1 \times 10^6$ yr and $\dot{P}_{2853} \approx 1 \times 10^{-11}$ s s^{-1}. A measurement of $\dot{P}$ for the 2853.8 μHz variation will indicate whether it is related to the 1902.5 μHz power or is an independent variation. Finally, theoretical work on the effects of tidal driving and accretion on a DB pulsator are imperative.

This work was supported in part by NSF grants AST 85-52456, AST 86-00507, AST 87-12249, AST 88-13572, AST 90-013978, AST 90-9013368, and AST 92-17988, NASA grant NGG-50468, National Geographic Society grant 3547-87, the NSERC of Canada, the fund FCAR (Quebec), and the Science and Engineering Research Council (UK). We are grateful to the participants of the Whole Earth Telescope for their time and efforts in producing unprecedented light curves, and thank Marion Frueh for her efforts at McDonald Observatory.

REFERENCES

Angel, J. R. P., & Landstreet, J. D. 1970, ApJ, 162, L61
Becker, R. H. 1981, ApJ, 251, 626
Bracewell, R. N. 1965, Fourier Transform and Its Application (New York: McGraw-Hill)
Bradley, P. A. 1993, Ph.D. thesis, Univ. Texas
Faulkner, J., Flannery, B. P., & Warner, B. 1972, ApJ, 175, L79 (FFW)
Frank, J., King, A. R., & Raine, D. J. 1985, Accretion Power in Astrophysics (Cambridge: Cambridge Univ. Press)
Greenstein, J., & Matthews, M. S. 1957, ApJ, 105, 85
Hirose, M., & Osaki, Y. 1990, PASJ, 42, 135
Humason, M. L., & Zwicky, F. 1947, ApJ, 105, 85
Kepler, S. O., et al. 1991, in NATO ASI Ser. Proc. Seventh European Workshop on White Dwarfs, ed. G. Vauclair & E. M. Sion (Dordrecht: Kluwer), 143
Kurtz, D. W., Shibahashi, H., & Goode, P. R. 1990, MNRAS, 247, 558
Lazaro, C., Solheim, J. E., & Arevalo, M. J. 1989, in IAU Colloq. 114, White Dwarfs, ed. G. Wegner (Berlin: Springer), 458
Marsh, T. R., & Horne, K. 1991, ApJ, 366, 535
Meyer, F., & Meyer-Hoffmeister, E. 1984, A&A, 140, L35
Nather, R. E. 1973, Vistas Astron., 15, 91
Nather, R. E., Winget, D. E., Clemens, J. C., Hansen, C. J., & Hine, B. P. 1990, ApJ, 361, 309
Patterson, J., Halpern, J., & Shambrook, A. 1993, ApJ, 419, 803
Patterson, J., Nather, R. E., & Robinson, E. L. 1979, ApJ, 232, 819
Patterson, J., Sterner, E., Halpern, J. P., & Raymond, J. C. 1992, ApJ, 384, 234
Provencal, J. L. 1993, Ph.D. thesis, Univ. Texas
Smak, J. 1967, Acta Astron., 17, 255
Solheim, J. E. 1989, in IAU Colloq. 114, White Dwarfs, ed. G. Wegner (Berlin: Springer), 446
———. 1994, private communication
Solheim, J. E., Robinson, E. L., Nather, R. E., & Kepler, S. O. 1984, A&A, 135, 1
Unno, W., Oskai, Y., Ando, H., Saio, H., & Shibahashi, H. 1989, Nonradial Oscillations of Stars (2d ed.; Tokyo: Univ. Tokyo Press)
Warner, B. 1986, MNRAS, 219, 347
Warner, B., & Robinson, E. L. 1972, MNRAS, 159, 101
Winget, D. E., & Fontaine, G. 1982, in Pulsations in Classical and Cataclysmic Variable Stars, ed. J. P. Cox & C. J. Hansen (Boulder: Univ. Colorado Press), 46
Winget, D. E., et al. 1994, ApJ, 430, 839
Winget, D. E., et al. 1991, ApJ, 378, 326
Winget, D. E., Nather, R. E., & Hill, J. A. 1987, ApJ, 316, 305
Zhang, E., Robinson, E. L., Ramseyer, T. F., Shetrone, M. D., & Steining, F. 1991, ApJ, 320, 714